Who's On First In 5G Mobile Networks: Equalizers or Polarization Diversity Combiners?

Farah Arabian, Michael Rice
Dept. Electrical & Computer Engineering
Brigham Young University
Provo, UT USA
farah.arabian@byu.edu, mdr@byu.edu

Rose Qingyang Hu
Dept. Electrical & Computer Engineering
Utah State University
Logan, UT, USA
rose.hu@usu.edu

***Abstract*—This paper studies combine-then-equalize and equalize-then-combine receiver architectures in a multicarrier scenario motivated by 5G cellular systems. The BER performance of these two receiver architectures with polarization diversity is compared. The results show that the combine-then-equalize approach better exploits the inherent diversity in the system.**

I. Introduction

Diversity is necessary to develop 5G system capacity. Diversity can be obtained in many ways, such as MIMO transmission and reception, spatial diversity, and polarization diversity. Polarization diversity has the advantage of small volume: it may be achieved using a pair of co-located orthogonally-polarized antenna elements. The performance of polarization diversity reception highly depends on how uncorrelated the outputs of the two antenna elements are [1], [2]. Multiple reflections between the transmitter and receiver tend to decorrelate the outputs of the two antenna elements [2], but not completely [1]. Despite the lack of complete decorrelation, it is possible to realize performance gains using polarization diversity [2].

The potential advantage for polarization diversity gains occurs in multipath propagation, where wideband signals experience frequency-selective fading. Equalization is the most common method used to address frequency-selective fading [3]. Thus, any study of polarization diversity should also investigate simultaneous equalization. This raises the question of how to order combining and equalization: which one should come first in order to achieve the best bit error rate performance?

5G systems probably will use multi-carrier modulations [4], [5]. The current LTE waveform is based on cyclic prefix orthogonal frequency division multiplexing (CP-OFDM), but 5G systems may generalize to Filter Bank Multi-Carrier (FBMC), Universal Filtered Multi-carrier (UFMC), etc. [4] to deal with the traditional OFDM drawbacks [6]. However all the multi-carrier modulations have some common disadvantages such as high peak to average power ratio (PAPR) and high side-lobes in the frequency domain. But because multicarrier modulations are more resistant to the frequency selective fading and conveniently accommodate multiplexing users with different data rates, multicarrier modulation is still favored for use in 5G systems.

Combining the outputs of multiple antennas in an OFDM system has been described in [7] – [11]. In [7], the relationship between selection combining (SC), equal gain combining (EGC), and maximum ratio combining (MRC) for single-carrier modulations in frequency non-selective fading, and the same combining techniques for OFDM were developed. Mathematical expressions for the bit error probability for simple single-carrier modulations in Rayleigh fading were shown to apply to the combined outputs after the FFT operation in an OFDM receiver. The work in [8] reduced the number of required FFT operations by introducing a pre-FFT combining technique involving two or more consecutive OFDM symbols. Post-FFT combining was examined in [9] where the best performing system applied a separate post-FFT frequency domain equalizer to each antenna branch and combined the equalizer outputs using MRC. The equalizers were applied before the combiner to facilitate the computation of soft information for a decoder. A similar arrangement (equalize-then-combine) was described in [10]. Here, the goal was optimum demodulation/decoding for *independent* channels on the antenna branches. The optimum process creates soft bit metrics, combines the soft information, then decodes. The creation of soft bit metrics implies an equalizer. In [11], pre-FFT combining and post-FFT combining were evaluated. The pre-FFT combining took the form of a beam former and MRC was applied to the bank of parallel FFT outputs. Equalization was explicitly mentioned only once in a comment that an equalizer could replace the combiner in the hardware prototype described in the paper. This leaves the reader with the impression that it was assumed that the pre-FFT beamformer removed the frequency selectivity of the channel.

This summary shows that none of the prior works considered polarization diversity (where the channels are not independent) or the ordering of combining and equalization. The published analyses of coded systems suggested that the preferred order is equalize-then-combine. For the uncoded systems considered in this paper, we show that combine-then-equalize is better. To the authors' knowledge, the only work to consider the ordering of combining and equalization was performed in [12] for $\pi/4$-DQPSK. The equalizer was an adaptive decision-feedback equalizer. Five systems were considered. The simulation results showed that equalization

978-1-7281-4291-3/20/$31.00 ©2020 IEEE

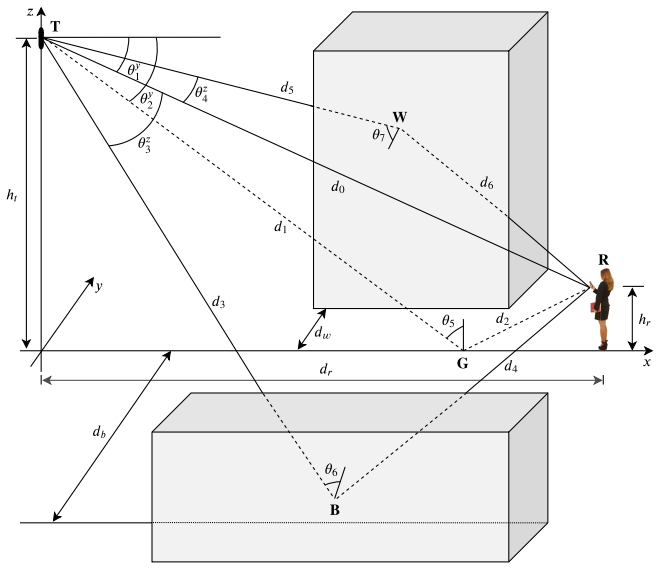

Fig. 1. An illustration of the 4-path multipath channel with polarization state information used in this paper.

followed by SC was better than SC followed by equalization. However, the best performing system applied separate feed-forward equalizer filters to the two antenna branches, combined the outputs of the two feed-forward filters, then applied decision-feedback to the combined signal. This is close to the combine-then-equalize system that is shown to be the best in this paper.

This paper is organized as follows. In Section II system model is outlined. Two different receiver architectures are discussed in the Section III. We investigate the combine-then-equalize architecture with five different combining strategies followed by the equalize-then-combine architecture with four different combining strategies. Simulation results, presented in Section IV, show that the combine-then-equalize architecture leverages the diversity in the cross-polarized channels better than the equalize-then-combine architecture and achieves a lower bit error rate.

II. System model

The transmitter is a vertically polarized base station antenna to a mobile handset as shown in Figure 1. The propagation scenario is a down-link channel in an urban area comprising four propagation paths: one line-of-sight path and three reflections. One reflection is from the ground and the other two from the sides of two buildings on opposite sides of the street. This model is an extension of the three-path model used in [13]. The polarization state dependent impulse response is given by

$$h(t) = h_x(t)\hat{\mathbf{x}} + h_y(t)\hat{\mathbf{y}} + h_z(t)\hat{\mathbf{z}}, \tag{1}$$

where $\hat{\mathbf{x}}$, $\hat{\mathbf{y}}$, and $\hat{\mathbf{z}}$ are unit vectors in the x, y, z-coordinate system shown in Figure 1.

The spatial impulse responses are

$$\begin{aligned} h_x(t) &= \sum_{m=0}^{3} h_{x,m}\delta(t-\tau_m), \\ h_y(t) &= \sum_{m=0}^{3} h_{y,m}\delta(t-\tau_m), \\ h_z(t) &= \sum_{m=0}^{3} h_{z,m}\delta(t-\tau_m). \end{aligned} \tag{2}$$

For $h_t = 30\,\text{m}$, $h_r = 1.15\,\text{m}$, $d_r = 120\,\text{m}$, $d_b = 18\,\text{m}$, and $d_w = 2\,\text{m}$, the channel coefficients (to four decimal places) and the delays (to five significant digits) are

$$\begin{aligned} h_{x,0} &= 0.2338, \\ h_{x,1} &= 0.2268 + j0.0003, \\ h_{x,2} &= 0.0502 - j0.0031, \\ h_{x,3} &= 0.1787 + j0.0020, \\ h_{y,0} &= 0, \\ h_{y,1} &= -0.0065 + j0.0000, \\ h_{y,2} &= 0, \\ h_{y,3} &= 0.0096 - j0.0008, \\ h_{z,0} &= 0.9723, \\ h_{z,1} &= -0.9444 - j0.0011, \\ h_{z,2} &= -0.1936 + j0.0121, \\ h_{z,3} &= -0.7551 - j0.0072, \\ \tau_0 &= 411.40\,\text{ns}, \\ \tau_1 &= 411.61\,\text{ns}, \\ \tau_2 &= 413.26\,\text{ns}, \\ \tau_3 &= 428.54\,\text{ns}. \end{aligned} \tag{3}$$

For the purposes of illustration, we assume the co-located orthogonally-polarized antenna elements are aligned with the x- and z-axes (i.e., the mobile is vertical and is facing the base station). Consequently, the two channels at the outputs of the co-located orthogonally-polarized antenna elements are $h_1(t) = h_x(t)$ and $h_2(t) = h_z(t)$. The channel transfer functions are plotted in the top plot of Figure 2.

CP-OFDM transmission is assumed. At the transmitter, data bits map to QAM symbols to which zeros and pilots are added. Using I_k to denote the N 16-QAM symbols, zeros, and pilots that constitute the OFDM symbol, the output of the N-point inverse FFT block is

$$d_n = \sum_{k=0}^{N-1} I_k e^{j2\pi kn/N}, \quad 0 \le n < N. \tag{4}$$

Here, I_k amplitude modulates the k-th subcarrier at a discrete-time frequency of $2\pi k/N$. The subcarrier separation is $1/N$ cycles/sample. In the continuous-time domain, an OFDM symbol has a duration of T_s seconds. The subcarrier separation is $\Delta f = 1/T_s$ cycles/s to ensure orthogonality [4]. Adding a

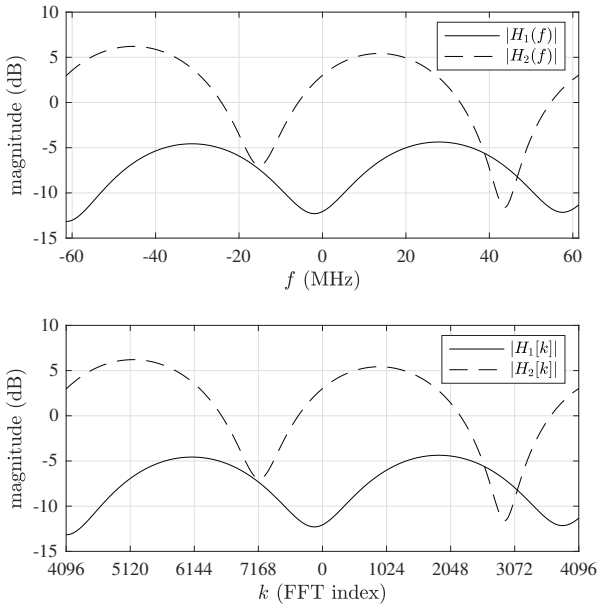

Fig. 2. The transfer functions of the two channels derived from orthogonally-polarized antenna elements in mobile handset. The first plot shows the channels as a function of frequency f. The second plot shows the channels as a function of FFT index.

cyclic prefix to the sequence d_n produces the sequence s_n. The complex-valued baseband equivalent of the OFDM symbol is

$$s(t) = \sum_n s_n g(t - nT), \tag{5}$$

where $g(t)$ is the pulse shape which we assume satisfies the Nyquist no-ISI condition, and $T = T_s/N$ s/sample. The cyclic prefix (CP) is inserted to account for the channel delay spread and makes linear convolution in the continuous-time domain look like circular convolution in anticipation of frequency domain equalization.

The complex baseband signal is transmitted from a linearly polarized transmit antenna through a frequency-selective multipath channel and received by an antenna in the mobile handset comprising co-located orthogonally polarized antenna elements. This is modeled as transmission through two parallel channels with impulse responses $h_1(t)$ and $h_2(t)$ with uncorrelated additive white Gaussian noise added to each channel. The two parallel received signals are passed through a pulse shape matched filters and sampled at T-spaced intervals. After removing the CPs on the two parallel paths, an N-point FFT is computed for each branch. At this point, the signal on branch m may be represented as

$$Y_m[k] = H_m[k]I_k + Z_m[k], \quad m = 1, 2, \tag{6}$$

where

$$H_m[k] = \begin{cases} H_m(k\Delta f) & 0 \le k \le N/2 - 1, \\ H_m((k-N)\Delta f) & N/2 \le k \le N - 1, \end{cases} \tag{7}$$

and where $Z_m[k]$ is a sequence complex-valued Gaussian random variables with zero mean and correlation function

$$\mathrm{E}\left\{Z_m[k+r]Z_m^*[k]\right\} = 2N_0\delta_r, \tag{8}$$

where δ_r is the Kronecker delta.

We consider the two post-FFT arrangements illustrated by the block diagrams in Figures 3 and 4. In Figure 3, the two parallel FFT outputs are combined and the combined signal is equalized. In Figure 4, the two parallel FFT outputs are independently equalized and the equalizer outputs are combined. The relative performances of these two approaches is the focus of this paper.

III. Detector Architectures

A. Combine Then Equalize

The detector shown in Figure 3 combines $Y_1[k]$ and $Y_2[k]$ then equalizes the combined sequence. The combined sequence is given by

$$Y[k] = C_1(k)Y_1[k] + C_2(k)Y_2[k], \quad 0 \le k < N. \tag{9}$$

The choice for the combining coefficients $C_1(k)$ and $C_2(k)$ defines the combining method:

- Selection Combining (SC): As in [7], we explore two versions of selection combining in this paper: (SC1) selects all of the subcarriers from one of the two channels and (SC2) selects the strongest subcarrier on a per-subcarrier basis. For SC1, the combining coefficients are

$$C_1(k) = \begin{cases} 1 & \sum_k |H_1[k]|^2 > \sum_k |H_2[k]|^2, \\ 0 & \text{otherwise}, \end{cases} \tag{10}$$

  for $0 \le k < N$. $C_2(k)$ is the complement of $C_1(k)$. For SC2, the combining coefficients are

$$C_1(k) = \begin{cases} 1 & |H_1[k]|^2 > |H_2[k]|^2 \\ 0, & \text{otherwise} \end{cases} \quad 0 \le k < N. \tag{11}$$

  $C_2(k)$ is the complement of $C_1(k)$.
- Equal Gain Combining (EGC): The combining coeffients are

$$C_1(k) = 1/2 e^{j\theta_1(k)}, \qquad C_2(k) = 1/2 e^{j\theta_2(k)}, \tag{12}$$

  for $0 \le k < N$. The phase angles $\theta_1(k)$ and $\theta_2(k)$ are required to co-phase the received signals before combining [14]. Again following [7], we explore two options for EGC in this paper: (EGC1) applies a constant phase shift across all subcarriers and (EGC2) applies a per-subcarrier phase shift. For EGC1, we use

$$\theta_1(k) = -\angle H_1[0], \qquad \theta_2(k) = -\angle H_2[0]. \tag{13}$$

  Here, the "phase" of the received signal is defined as the phase at the carrier frequency. For EGC2, we use

$$\theta_1(k) = -\angle H_1[k], \qquad \theta_2(k) = -\angle H_2[k]. \tag{14}$$

- Maximum Ratio Combining (MRC): For MRC, we use [11]

$$C_1(k) = \frac{H_1^*[k]}{|H_1[k]|^2 + |H_2[k]|^2}, \tag{15}$$

$$C_2(k) = \frac{H_2^*[k]}{|H_1[k]|^2 + |H_2[k]|^2}. \tag{16}$$

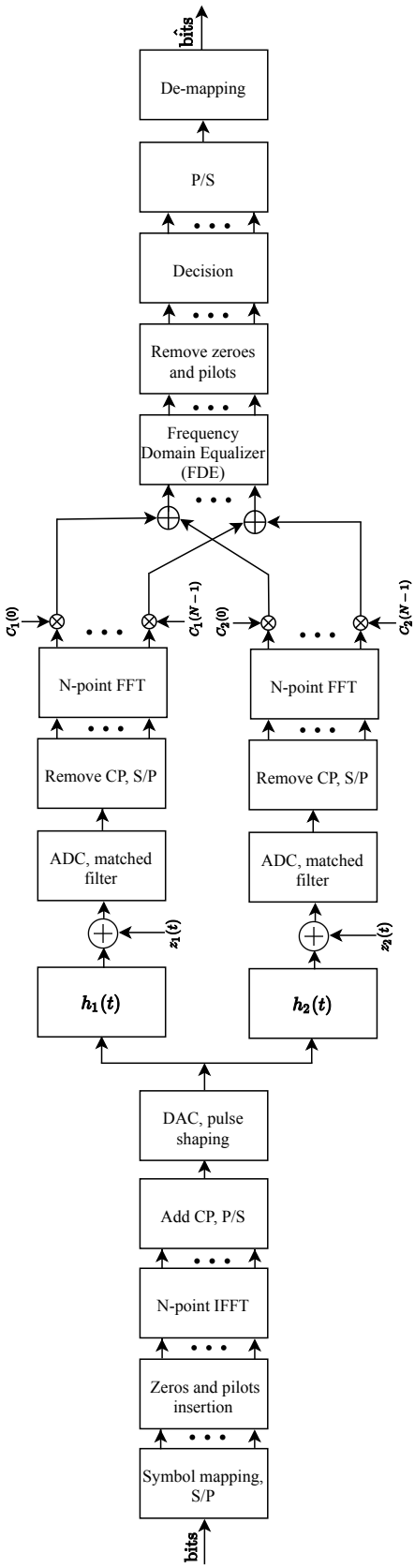

Fig. 3. Combine-then-equalize system architecture.

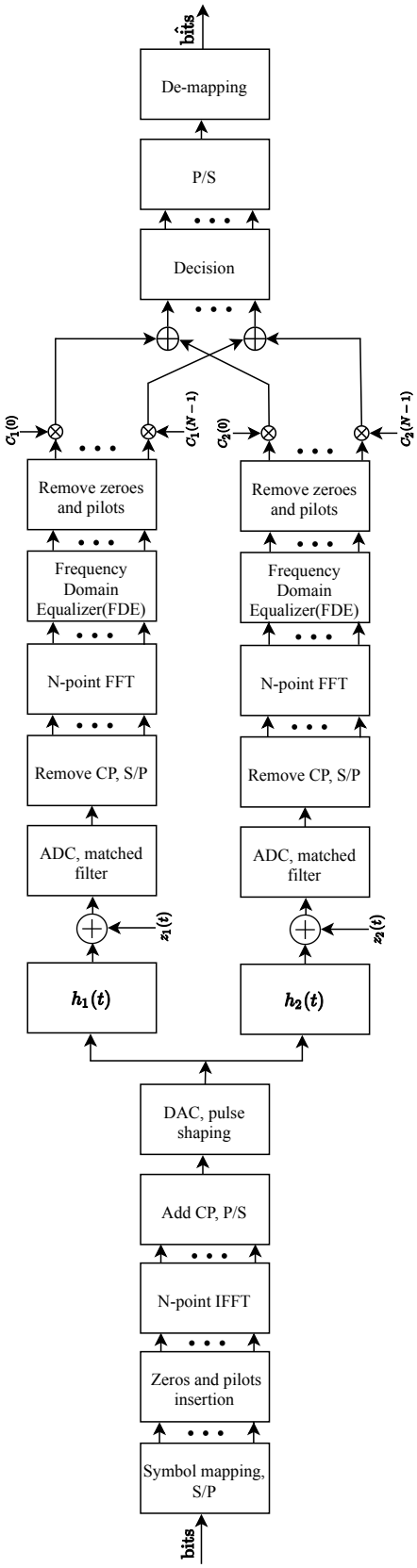

Fig. 4. Equalize-then-combine system architecture.

Note that in this case, the combining coefficients can be different for each subcarrier [7], [11]. No additional co-phasing is required here because the complex-valued combining coefficients align the phases of each subcarrier of $Y_1[k]$ and $Y_2[k]$.

The equivalent FFT-domain channel transfer function at the combiner output is

$$H[k] = C_1(k)H_1[k] + C_2(k)H_2[k], \quad 0 \le k < N. \tag{17}$$

After combining, an MMSE FDE is applied in the FFT domain. The MMSE equalizer is an LTI system with transfer function [3]

$$W[k] = \frac{H^*[k]}{|H[k]|^2 + S_n[k]}, \quad 0 \le k < N, \tag{18}$$

where $S_n[k]$ is the FFT-domain power spectral density of the noise after combining. The equalizer output $\hat{I}_k = Y[k]W[k]$ is used to produce the symbol estimate $\tilde{I}_k$. $\tilde{I}_k$ is de-mapped to produce an estimate of the bit sequence.

B. Equalize Then Combine

The detector shown in Figure 4 reverses the order of combining and equalization. Here, two equalizers are applied to $Y_1[k]$ and $Y_2[k]$ in parallel. The the equalizer outputs are combined to produce the input to the demapping. The two equalizers are MMSE equalizers operating on their respective channels:

$$W_1[k] = \frac{H_1^*[k]}{|H_1[k]|^2 + 2N_0}, \tag{19}$$

$$W_2[k] = \frac{H_2^*[k]}{|H_2[k]|^2 + 2N_0}, \tag{20}$$

and the equalizer outputs are

$$\hat{I}_{k,1} = Y_1[k]W_1[k], \tag{21}$$

$$\hat{I}_{k,2} = Y_2[k]W_2[k], \tag{22}$$

for $0 \le k < N$. The combined output is

$$\hat{I}_k = C_1(k)\hat{I}_{k,1} + C_2(k)\hat{I}_{k,2}. \tag{23}$$

The combining coefficients are determined by the combining method. No co-phasing is required when combining equalizer outputs because the equalizer has corrected the phase shifts caused by the channel.

- Selection Diversity (SC): As before two versions of selection combining are examined. The definitions of $C_1(k)$ and $C_2(k)$ are identical to those given in Section III-A.
- Equal Gain Combining (EGC): $C_1(k) = C_2(k) = 1/2$.
- Maximum Ratio Combining (MRC): The combining coefficients are set proportional to the pre-equalizer signal-to-noise ratio for each subcarrier which, for our purposes, is proportional to the magnitude squared of the channel coefficients:

$$C_1(k) = \frac{|H_1[k]|^2}{|H_1[k]|^2 + |H_2[k]|^2}, \tag{24}$$

$$C_2(k) = \frac{|H_2[k]|^2}{|H_1[k]|^2 + |H_2[k]|^2}. \tag{25}$$

TABLE I
PARAMETERS USED FOR THE BER SIMULATIONS.

Parameter	Variable	Value
QAM alphabet	–	16-QAM
Carrier frequency	f_0	3.7 GHz
Channel bandwidths	BW	100 MHz
Subcarrier spacing	Δf	15 kHz
Number of data subcarriers	–	4500
Number of pilot subcarriers	–	1500
FFT length	N	8192
Number of resource blocks	RB	500
Sampling rate	–	122.88 MHz

IV. SIMULATION RESULTS

Using the parameters listed in Table I, the bit error rate was simulated for the two systems outlined in Figures 3 and 4. The combiners and equalizers require the values of the channel transfer functions at the frequencies corresponding to the FFT bin centers. This mapping is illustrated in the bottom plot of Figure 2.

The simulated BER results for the combine-then-equalize system of Figure 3 are plotted in Figure 5. The results show that EGC (both versions) and MRC have similar performance and that both are better than both versions of SC. The similar performance of EGC and MRC was also observed in [7] and is explained by the fact that when the two channels derive from co-located orthogonally-polarized antenna elements, the two channels are rarely equal power. The antenna that is closer to being co-polarized with the transmit antenna generally experiences the stronger channel. In this example, $h_z(t)$ is co-polarized with the transmit antenna (see Figure 1). Because our assignments are $h_1(t) = h_x(t)$ and $h_2(t) = h_z(t)$, $h_2(t)$ is stronger than $h_1(t)$ [see Figure 2]. The signal-to-noise ratios at the outputs of the two antenna elements are within about 10 dB of each other. This is not an extreme case; and for the signal-to-noise ratios of interest, MRC is only slightly-better than EGC. As the difference between the signal-to-noise ratios of the two channels increases, MRC exhibits increasing performance gains over EGC. It is also observed that EGC with per-subcarrier co-phasing (EGC2) is slightly better than EGC with a constant co-phasing (EGC1).

Moving to the SC results, observe at SC2 is superior to SC1. SC2 has the advantage of selecting the contribution from the strongest of the two channels on a per-subcarrier basis. Close examination of the channels in Figure 2 shows that for most subcarriers, SC2 selects $Y_2[k]$. But for subcarriers $2588 \le k \le 3113$, SC2 selects $Y_1[k]$. Consequently SC2 leverages the diversity present in the two channels better than SC1.

The simulated BER results for the equalize-then-combine system of Figure 4 are plotted in Figure 6. The normal ordering (MRC is superior to EGC which is superior to SC) is observed, *except* for SC2. Here SC2 leverages the diversity available in the channel better than SC1, EGC, and MRC for low signal-

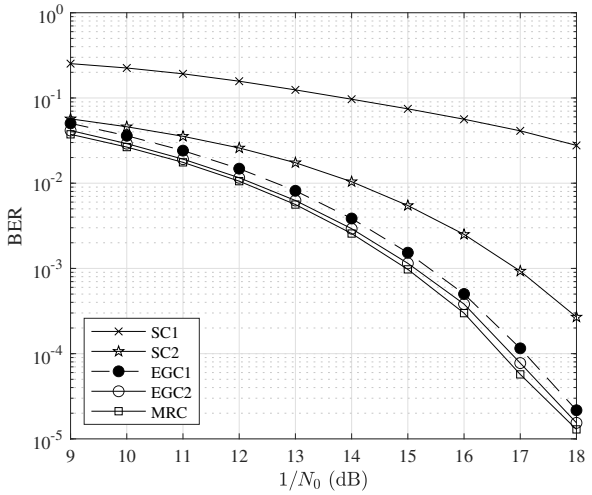

Fig. 5. The simulated BER performance of the combine-then-equalize system of Figure 3 for five different combining techniques outlined in Section III-A.

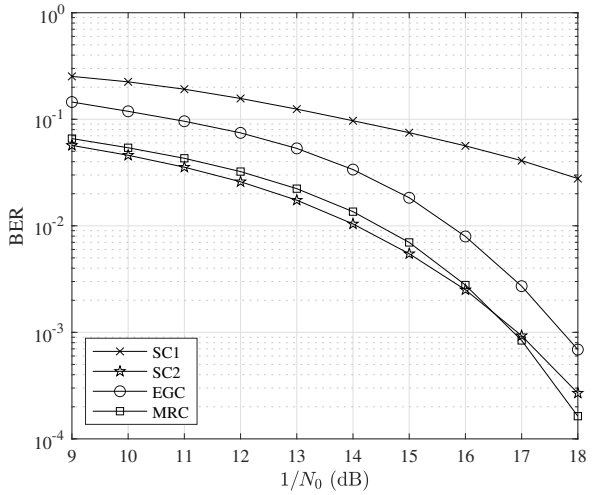

Fig. 6. The simulated BER performance of the equalize-then-combine system of Figure 4 for the four different combining techniques outlined in Section III-B.

to-noise ratios. This is explained as follows. Because both $H_1[k]$ and $H_2[k]$ display spectral nulls, the two equalizers produce noise enhancement at their respective FFT indexes corresponding to those nulls. The EGC and MRC combine this enhanced noise from both equalizer outputs to form the input to the decision block. In contrast, SC2 passes to the decision block enhanced noise from one of the two equalizer outputs. The way the selection is performed, the noise enhancement is minimized. When the noise power is relatively high, the reduced noise output of SC2 dominates the BER performance. As the noise power diminishes, the behavior is less pronounced and the advantages of combining start to dominate.

What is interesting is that the best-performing option for the equalize-then-combine system (MRC) is worse than all the EGC and MRC curves for the combine-then-equalize system in Figure 5. This suggests that the combine-then-equalize system of Figure 3 more effectively exploits the diversity available from polarization diversity. In other words, equalizers benefit more from the signal-to-noise ratio gains due to combining. When the order is reversed, the noise enhancement that accompanies equalization reduces the signal-to-noise ratio improvement of the combiner.

V. Conclusion

In this paper, the BER performance of combine-then-equalize and equalize-then-combine systems with polarization diversity is compared in a multicarrier scenario motivated by 5G cellular systems. A static downlink channel with polarization state information is used in this comparison. The channel was derived from a ray-tracing analysis in an urban scenario. The results show that the combine-then-equalize approach better exploits the inherent diversity in the system.

References

[1] W. Lee and Y. Yeh, "Polarization diversity for mobile radio," *IEEE Transactions on Communications*, vol. 20, pp. 913–923, October 1972.

[2] R. Vaughan, "Polarization diversity in mobile communications," *IEEE Transactions on Vehicular Technology*, vol. 39, pp. 177–186, August 1990.

[3] J. Proakis and M. Salehi, *Digital Communications*. New York: McGraw-Hill, 5th ed., 2007.

[4] Y. Cai *et al.*, "Modulation and multiple access for 5G networks," *IEEE Communications Surveys & Tutorials*, vol. 20, pp. 629 – 646, First quarter 2018.

[5] Rohde & Schwarz Inc., "5G waveform candidates," June 2016. Available at http://www.rohde-schwarz.com/appnote/1MA271.

[6] S. Nagul and V. Nagar, "A review on 5G modulation schemes and their comparisons for future wireless communications," in *Proceedings of the IEEE Conference on Signal Processing And Communication Engineering Systems (SPACES)*, (Vijayawada, India), 4-5 January 2018.

[7] D. Lee, G. Saulnier, Z. Ye, and M. Medley, "Antenna diversity for an OFDM system in a fading channel," in *Proceedings of the IEEE Communications Conference*, (Atlantic City, NJ), pp. 1104–1109, 31 October - 3 November 1999.

[8] S. Slimane, "A low complexity antenna diversity receiver for OFDM based systems," in *Proceedings of the IEEE International Conference on Communications*, (Helsinki, Finland), pp. 1147–1151, 11-14 June 2001.

[9] A. Dammann and S. Kaiser, "Standard conformable antenna diversity techniques for OFDM and its application to the DVB-T system," in *Proceedings of the IEEE Global Telecommunications Conference*, (San Antonio, TX), pp. 3100–3105, 25–29 November 2001.

[10] X. Ouyang, M. Ghosh, and J. Meehan, "Optimal antenna diversity combining for IEEE 802.11a system," *IEEE Transactions on Consumer Electronics*, vol. 48, pp. 738 – 742, August 2002.

[11] D. Pham *et al.*, "Implementation of joint pre-FFT adaptive array antenna and post-FFT space diversity combining for mobile ISDB-T receiver," *IEICE Transactions on Communications*, vol. 91-B, pp. 127–138, January 2008.

[12] Q. Liu, K. Scott, Y. Wan, and A. Sendyk, "Performance of decision-feedback equalizers with dual antenna diversity," in *Proceedings of the IEEE Vehicular Technology Conference*, (Secaucus, NJ, USA), pp. 637–640, 18-20 May 1993.

[13] F. Arabian, G. P. Nordin, and M. Rice, "On polarization dependent equalization in 5G mmWave systems," in *2020 International Conference on Computing, Networking and Communications (ICNC)*, pp. 1058–1062, 2020.

[14] A. Molisch, *Wireless Communications*. West Sussex, UK: John Wiley & Sons Ltd. for IEEE Press, second ed., 2011.